Determination of Cloud Optical Thickness Over Snow Using Satellite Measurements in the Oxygen A-Band

Cornelia Schlundt, Alexander A. Kokhanovsky, Vladimir V. Rozanov, and John P. Burrows

***Abstract*—We present our newly developed Cloud optical thickness Retrieval Over Snow (CROS) algorithm, which makes use of the sensitivity of top-of-atmosphere (TOA) reflectance in the oxygen A-band to the cloud optical thickness. The CROS algorithm applies forward simulations for clouds over snow using the radiative transfer model SCIATRAN in order to find the cloud optical thickness (and cloud bottom height and effective underlying surface albedo) representing the measured TOA radiance for a given cloud top height and solar zenith angle. We present results for synthetic retrievals as well as an error analysis with respect to errors in cloud top height. It was demonstrated that the retrievals are most robust for thin high clouds. The retrievals for low-level clouds require an accurate estimation of the cloud altitude ahead of the cloud optical thickness retrieval. Also, it is demonstrated that the retrievals become less accurate for the cases of low Sun.**

***Index Terms*—Radiative transfer, remote sensing.**

I. Introduction

CLOUDS are the subject of interest for numerical weather prediction models, global circulation models, and climate studies. Due to the fact that clouds vary considerably in their horizontal and vertical extent, which is crucial to studies of global climate change, it is of great importance to have a good knowledge on cloud properties and their variation in space and time. One of the most relevant parameters for such studies is the cloud optical thickness because short-wave cloud radiative properties depend almost exclusively on this parameter. Currently, there is no retrieval algorithm capable of determining the cloud optical thickness over snow surfaces since such targets appear as bright as clouds in the visible wavelength region. One possibility is to use measurements at wavelengths of 1.24, 1.6, 2.1, and 3.7 μm for the determination of cloud optical thickness and effective radius [1]. This is because snow appears darker at these wavelengths as compared to the visible spectral range. However, photons do not penetrate deep into clouds in the near infrared spectral range. Therefore, the method is applicable only to thin clouds. In this letter, we propose to use measurements in the oxygen A-band for the determination of cloud optical thickness provided that the cloud top height is derived from independent measurements. The algorithm and its application to synthetic data are presented.

Manuscript received August 11, 2012; revised October 1, 2012 and December 5, 2012; accepted December 13, 2012. Date of publication February 6, 2013; date of current version June 13, 2013.

The authors are with the Institute of Environmental Physics and Remote Sensing, University of Bremen, 28334 Bremen, Germany (e-mail: alexk@iup.physik.uni-bremen.de).

Color versions of one or more of the figures in this paper are available online at http://ieeexplore.ieee.org.

Digital Object Identifier 10.1109/LGRS.2012.2234720

This letter is organized as follows. First, we discuss the cloud reflectance in the oxygen A-band, which is the gaseous absorption band of interest in this study. Then, an explanation of the radiative transfer model (forward model) is given with respect to the most relevant model settings followed by a description of the retrieval algorithm (inverse model). Afterward, the retrieval results of the algorithm are discussed.

II. Theory

A. Forward Model

We investigate the cloud reflectance over a snow surface in the oxygen A-band (758–771 nm) using the radiative transfer model SCIATRAN, which has been developed at Bremen University [2], [3]. The SCIATRAN model stems from the well-known GOMETRAN model (radiative transfer model for the Global Ozone Monitoring Experiment (GOME) instrument) highly used in trace gas retrievals [4] and is aimed at the interpretation of measurements of SCanning Imaging Absorption spectroMeter for Atmospheric CHartographY (SCIAMACHY) on board ENVIronmental SATellite (ENVISAT) [5]. The development of the SCIATRAN code started in 2000 and now became a comprehensive software package for the simulation of radiative transfer in the terrestrial atmosphere in the spectral range from ultraviolet to the thermal infrared including polarization and ocean–atmosphere coupling.

In this letter, we use the discrete ordinate technique for the numerical solution of the radiative transfer equation ignoring polarization. A comparison study (not shown here) of results derived from the vector and scalar discrete ordinate technique led to the conclusion that the scalar mode of SCIATRAN is sufficient for modeling the scenario of an optically thick cloud located over a snow surface neglecting polarization effects since the maximum difference amounts to $\sim$0.1%.

We assume scattered light in a plane-parallel atmosphere in order to simulate synthetic radiances as they would be measured by SCIAMACHY. Therefore, the half width half maximum (HWHM) of the spectral response function is needed for the convolution of each spectral point. We assume a Gaussian HWHM of 0.24 nm corresponding to SCIAMACHY channel 4 (595–812 nm), where the oxygen A-band is located. This band is important for the cloud-top-height determination from spaceborne instruments and is commonly used in cloud retrieval algorithms [6], [7].

Moreover, multiple scattering including Delta-M truncation and single scattering correction are considered in SCIATRAN. The single scattering correction technique allows to reduce

the error introduced by the truncation of the phase function representation (see [8] for details and references therein).

Aerosol properties are taken from the World Meteorological Organization model with respect to the size distribution and spectral refractive index of respective components. It is assumed that sizes of particles are distributed according to the lognormal law [9]. Four aerosol layers are considered in the radiative transfer model. The boundary layer model used corresponds to the case of maritime aerosol, while the tropospheric aerosol model is related to the case of continental aerosol. The stratospheric and mesospheric aerosol models used correspond to the background aerosol.

Performing radiative transfer calculations, we have assumed that an ice cloud is represented by ice crystals, which are modeled as Koch fractals of the second generation on the basis of a regular tetrahedron having a size of 100 μm. The snow surface is modeled as an optically thick ice cloud (optical thickness equal to 5000) on the ground having a geometrical thickness of 1 m. Thus, the bidirectional reflection distribution function of snow is taken into account instead of assuming a Lambertian surface. Fig. 1 shows modeled SCIAMACHY top-of-atmosphere (TOA) reflectances as a function of wavelength representing low-level ($h_b = 1$ km and $h_t = 3$ km) (1a), mid-level ($h_b = 5$ km and $h_t = 7$ km) (1b), and high-level ($h_b = 9$ km and $h_t = 11$ km) (1c) ice clouds with different cloud optical thicknesses (τ) over snow at nadir and solar zenith angle (ϑ_0) equal to 60°. h_b and h_t denote the cloud bottom height and cloud top height, respectively. In all cases shown, it is obvious that there is no sensitivity of solar light reflectance to τ outside of the O_2 A-band (758 nm), which is different to the situation inside of the O_2 A-band (761 nm), where the sensitivity of the reflectance to the value of τ is increasing with increasing cloud height. In Fig. 2, we replaced the underlying snow layer by a black surface (e.g., ocean) and modeled SCIAMACHY TOA reflectances for the same ice cloud scenarios as shown in Fig. 1 in order to demonstrate that the spectral behavior is changing significantly with respect to the sensitivity of reflectance to the value of cloud optical thickness, particularly outside of the O_2 A-band, for the case of a snow-free surface.

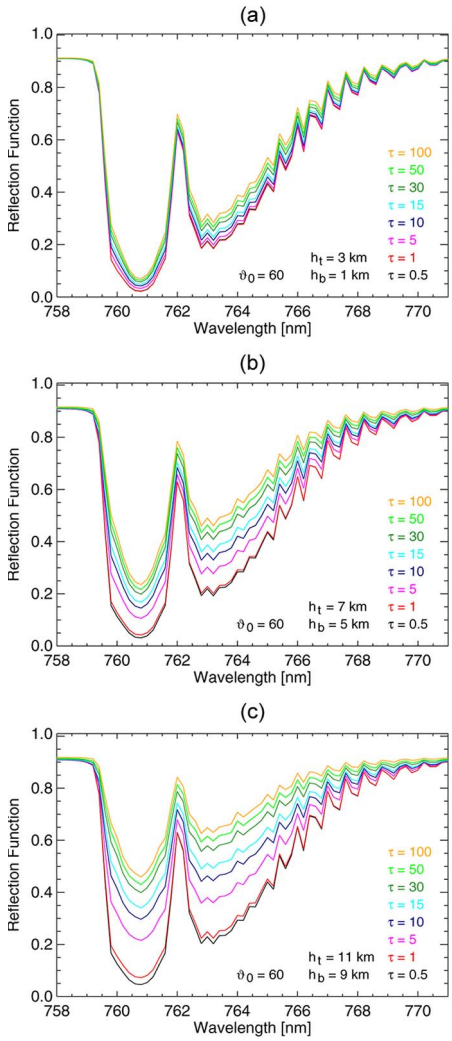

Fig. 1. Modeled SCIAMACHY TOA reflectances as a function of wavelength representing (a) low-level, (b) midlevel, and (c) high-level ice clouds for different cloud optical thicknesses (τ) over snow at nadir and solar zenith angle (ϑ_0) equal to 60°. h_b and h_t denote the cloud bottom height and the cloud top height, respectively. For interpretation of colors, please see online version.

B. Retrieval Algorithm

In this letter, we assume that the cloud top height and the thermodynamic state of the cloud are known from independent measurements (lidar and radar). Then, the suggested algorithm [Cloud optical thickness Retrieval Over Snow (CROS)] is capable to retrieve the cloud optical thickness, the cloud bottom height, and the effective albedo of the surface simultaneously. The CROS algorithm consists of two parts.

The first part deals with the linearization of the radiative transfer forward model in order to find the linear relationship between the variation of intensity I (or radiance) and the variation of the cloud bottom height h_b, cloud optical thickness τ, and effective albedo A (see [10] for details). This is done by using the following equation:

$$\delta I(\lambda, \Omega) = W_\lambda^{h_b}(\Omega) \cdot \delta h_b + W_\lambda^{\tau}(\Omega) \cdot \delta\tau + W_\lambda^{A}(\Omega) \cdot \delta A \quad (1)$$

with $\Omega = (\mu_0, \mu, \varphi - \varphi_0)$. μ_0 denotes the cosine of the solar zenith angle, μ is the cosine of the viewing zenith angle, and φ_0 is the azimuth angle. $W_\lambda^{h_b}$, W_λ^{τ}, and W_λ^{A} are derivatives of the intensity with respect to h_b, τ, and A. These are the so-called weighting functions. The calculation of weighting functions is based on the simultaneous solution of forward and adjoint radiative transfer equations as described in [11]. Fig. 3 displays the weighting functions of the cloud optical thickness (red), cloud bottom height (blue), cloud top height (orange), and effective albedo (green) for the same ice cloud scenarios as shown in Fig. 1 above snow ($A = 0.9$) at nadir view and $\vartheta_0 = 60°$. In the previous section, we already mentioned the insensitivity of the solar light reflectance to the value of cloud optical thickness outside of the O_2 A-band in the case of a snow surface below a cloud, which is also demonstrated in Fig. 3(a)–(c) as its weighting function (W_λ^{τ}) is almost zero at 758 nm. Furthermore, the derivatives of the intensity with respect to h_b and h_t are also zero in that spectral region, and thus, the retrieval algorithm is insensitive here to the cloud position. Based on the fact that W_λ^{τ}, $W_\lambda^{h_b}$, and W_λ^{A} exhibit different spectral behavior patterns inside of the O_2 A-band, the algorithm is capable to retrieve all three parameters simultaneously. It is important to note that the algorithm is not able to determine h_b and h_t simultaneously because their weighting functions are very similar over the

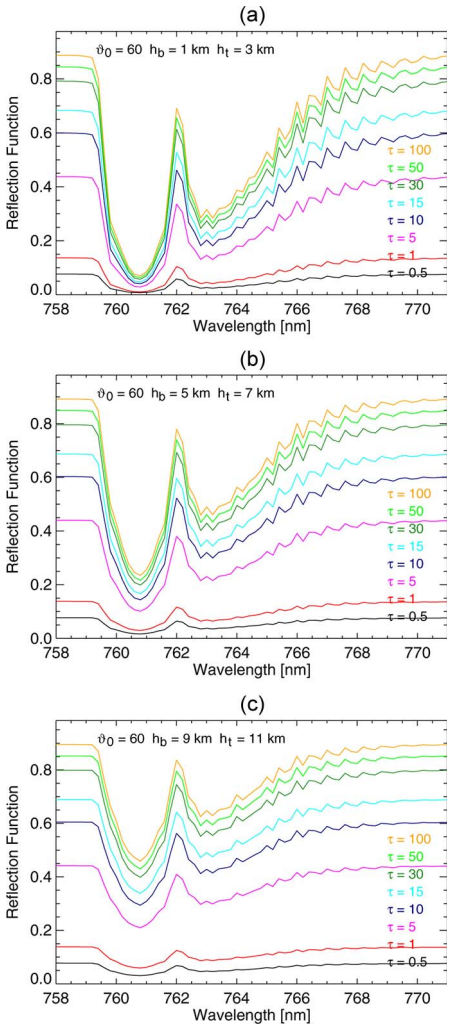

Fig. 2. Modeled SCIAMACHY TOA reflectances as a function of wavelength representing (a) low-level, (b) midlevel, and (c) high-level ice clouds for different cloud optical thicknesses (τ) over a black surface (e.g., ocean) at nadir and solar zenith angle (ϑ_0) equal to 60°. h_b and h_t denote the cloud bottom height and the cloud top height, respectively. For interpretation of colors, please see online version.

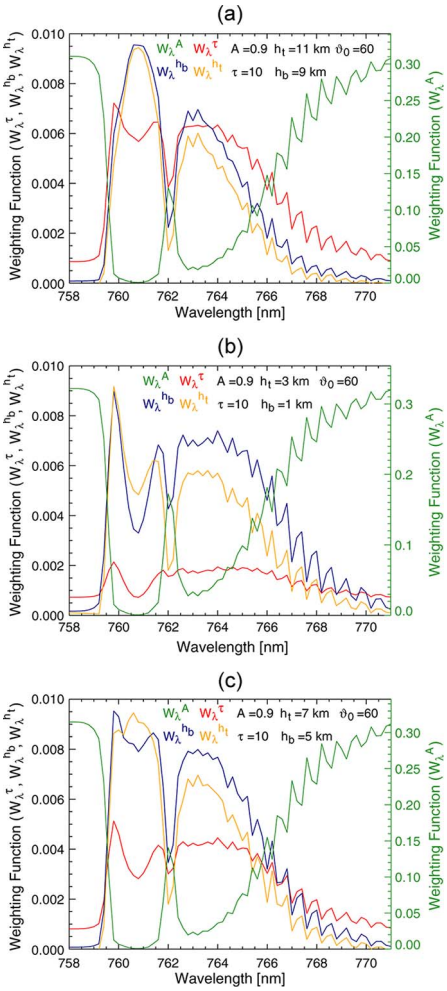

Fig. 3. Weighting functions of (red) cloud optical thickness W_λ^τ, (blue) cloud bottom height $W_\lambda^{h_b}$, (orange) cloud top height $W_\lambda^{h_t}$, and (green) effective albedo W_λ^A for (a) low-level, (b) midlevel, and (c) high-level ice clouds ($\tau = 10$) above snow (albedo $= 0.9$) at nadir and solar zenith angle (ϑ_0) equal to 60°. $W_\lambda^{h_b}$ and $W_\lambda^{h_t}$ have the dimension [km^{-1}], while W_λ^τ and W_λ^A are dimensionless. For interpretation of colors, please see online version.

spectrum of interest. Additionally, it is worth mentioning that the whole simulated SCIAMACHY spectrum in the oxygen A-band (i.e., 66 spectral points) is used within the retrieval.

The second part is the solution of the inverse problem [12] based on the following equation:

$$\vec{Y} = \hat{\mathbf{A}} \cdot \vec{X} \tag{2}$$

with $\vec{Y}$ being the difference between the measured (in this study: synthetic) and modeled reflected light intensities, $\hat{\mathbf{A}}$ being the matrix containing the weighting functions for each spectral point, and $\vec{X}$ being the difference between the estimated and *a priori* assumed cloud bottom heights, cloud optical thicknesses, and effective albedo. An analytical solution for $\vec{X}$ is found by minimizing the following quadratic form:

$$|\vec{Y} - \hat{\mathbf{A}} \cdot \vec{X}|^2 = \min . \tag{3}$$

III. Results

We have performed retrievals using synthetic data simulating nadir SCIAMACHY measurements. The radiative transfer runs were done with the radiative transfer model SCIATRAN. For the model study, six different ice clouds over snow scenarios are considered: low-level ($h_b = 1$ km), midlevel ($h_b = 5$ km), and high-level ($h_b = 9$ km) cloud, each having a geometrical thickness of $\Delta G = 1$ km and $\Delta G = 2$ km, respectively. For the generation of the synthetic data set, the snow surface (1 m) is modeled as an optically thick ice cloud ($\tau = 5000$) on the ground including multiple scattering processes. However, in the retrieval process, a simple Lambertian surface is assumed instead of the unknown spectral surface reflectance of snow, demonstrating that the algorithm is robust with respect to the underlying snow layer properties.

Figs. 4(a), 5(a), and 6(a) show for each of the six cases mentioned earlier the averaged sensitivity of the modeled SCIAMACHY TOA reflectances between 760.4 and 761.2 nm, i.e., where the maximum of the oxygen absorption occurs, as a function of cloud optical thickness (0.1–100) and solar zenith angle (0°, 15°, 30°, 45°, 60°, and 75°). Figs. 4(b), 5(b), and 6(b) and Figs. 4(c), 5(c), and 6(c) present the retrieval results for $\vartheta_0 = 60$, nadir observation, and τ ranging between 5 and 50, for $\Delta G = 1$ km and $\Delta G = 2$ km, respectively.

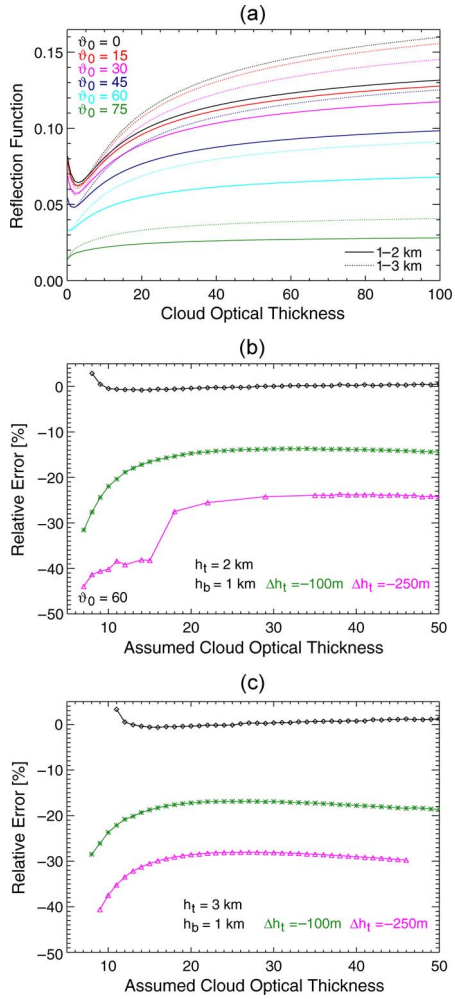

Fig. 4. Low-level ice cloud over snow ($h_b = 1$ km) having a geometrical thickness of $\Delta G = 1$ km and $\Delta G = 2$ km, respectively. (a) shows the averaged sensitivity of the TOA radiance between 760.4 and 761.2 nm (maximum of O_2 A-band) as a function of cloud optical thickness (τ) and solar zenith angle (ϑ_0). (b) and (c) present the retrieval results of CROS ranging between $\tau = 5$ and $\tau = 50$ for $\vartheta_0 = 60°$ and for $\Delta G = 1$ km and $\Delta G = 2$ km, respectively. In order to demonstrate the robustness of the algorithm, we have introduced an error in cloud top height: $\Delta h_t = \pm 100$ m and $\Delta h_t = \pm 250$ m. For interpretation of colors, please see online version.

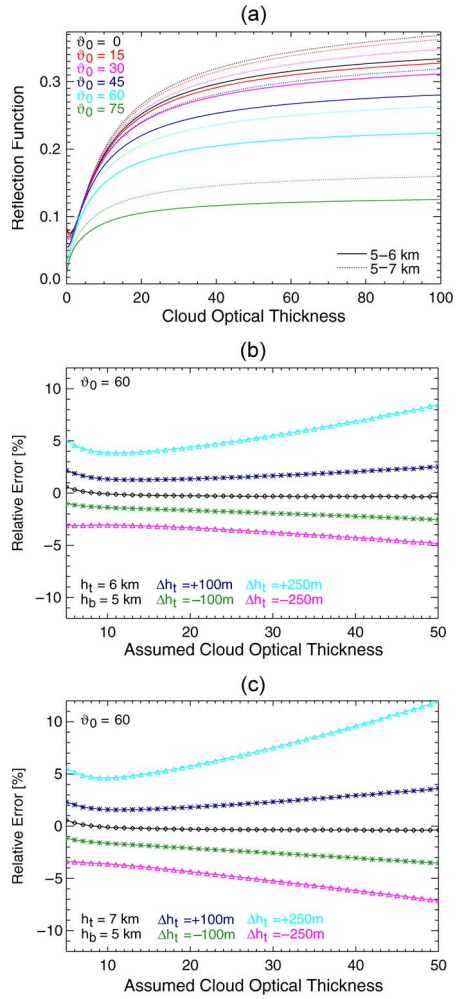

Fig. 5. Mid-level ice cloud over snow ($h_b = 5$ km) having a geometrical thickness of $\Delta G = 1$ km and $\Delta G = 2$ km, respectively. (a) shows the averaged sensitivity of the TOA radiance between 760.4 and 761.2 nm (maximum of O_2 A-band) as a function of cloud optical thickness (τ) and solar zenith angle (ϑ_0). (b) and (c) present the retrieval results of CROS ranging between $\tau = 5$ and $\tau = 50$ for $\vartheta_0 = 60°$ and for $\Delta G = 1$ km and $\Delta G = 2$ km, respectively. In order to demonstrate the robustness of the algorithm, we have introduced an error in cloud top height: $\Delta h_t = \pm 100$ m and $\Delta h_t = \pm 250$ m. For interpretation of colors, please see online version.

In order to demonstrate the robustness of CROS, we introduced an error in cloud top height: $\Delta h_t = \pm 100$ m and $\Delta h_t = \pm 250$ m. The symbols (diamonds, stars, and triangles) represent retrieval results where the algorithm converged. We have used the threshold of 1% as the convergence criterion.

By comparing the retrieval results derived for all six scenarios (see Figs. 4–6), one can see that the sensitivity of the algorithm is increasing with increasing cloud bottom height, decreasing cloud optical thickness, and decreasing solar zenith angle. The relative error is smallest (< 2–3%) for high-level ice clouds above snow (see Fig. 6), whereas it is biggest ($< 40\%$) for low-level ice clouds (see Fig. 4). In particular, the convergence was not reached for the error in cloud top height of 100 and 250 m in the case of low-level clouds. Therefore, the corresponding retrieval results are absent in Fig. 4(a) and (b). Additionally, we present in Fig. 7 the results for cloud bottom height, which are simultaneously retrieved with cloud optical thickness, for each of the six cloud cases. The errors of the retrieved cloud bottom height are larger as compared to the errors in cloud optical thickness. However, the cloud bottom height is only a by-product of the retrieval algorithm.

IV. Conclusion

This theoretical study presents a newly developed retrieval algorithm, called CROS, for the determination of the cloud optical thickness of ice clouds above snow under the assumption that the cloud top height and the thermodynamic state of the cloud are known from independent measurements (e.g., lidar and radar).

We demonstrate that the algorithm is capable of retrieving simultaneously the cloud optical thickness, the cloud bottom height, and the effective albedo of snow using an optimal estimation approach. It provides accurate cloud optical thickness results for high-level clouds, reasonable results for midlevel clouds, and moderate results for low-level clouds. This is due to the fact that the sensitivity of the algorithm is decreasing with decreasing cloud bottom height, increasing solar zenith angle, and increasing cloud optical thickness. Furthermore, it

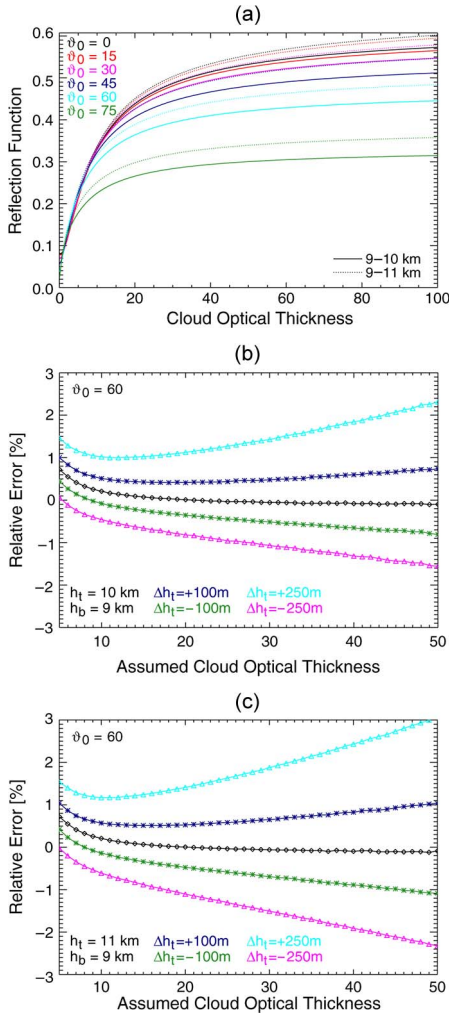

Fig. 6. High-level ice cloud over snow ($h_b = 5$ km) having a geometrical thickness of $\Delta G = 1$ km and $\Delta G = 2$ km, respectively. (a) shows the averaged sensitivity of the TOA radiance between 760.4 and 761.2 nm (maximum of O_2 A-band) as a function of cloud optical thickness (τ) and solar zenith angle (ϑ_0). (b) and (c) present the retrieval results of CROS ranging between $\tau = 5$ and $\tau = 50$ for $\vartheta_0 = 60°$ and for $\Delta G = 1$ km and $\Delta G = 2$ km, respectively. In order to demonstrate the robustness of the algorithm, we have introduced an error in cloud top height: $\Delta h_t = \pm 100$ m and $\Delta h_t = \pm 250$ m. For interpretation of colors, please see online version.

is shown that the algorithm is able to retrieve the cloud optical thickness above snow assuming in the retrieval process a simple Lambertian surface instead of the unknown realistic snow layer.

In the next step, the CROS algorithm for the determination of cloud optical thickness will be validated using real measurements derived from spaceborne or airborne/ground lidars and/or radars (for cloud top height altitude determination) and from spaceborne spectrometers such as SCIAMACHY on board ENVISAT (or GOME-2 on board Meteorological Operational Satellite). The algorithm can be also used for the analysis of cloud scenes sensed by other spectrometers such as the future European Space Agency Sentinel-4, Sentinel-5, and Sentinel-5p missions.

ACKNOWLEDGMENT

This work has been performed in the framework of the Deutsche Forschungsgemeinschaft REmote SensINg of aerosols, Clouds and trace gases (RESINC-2) project.

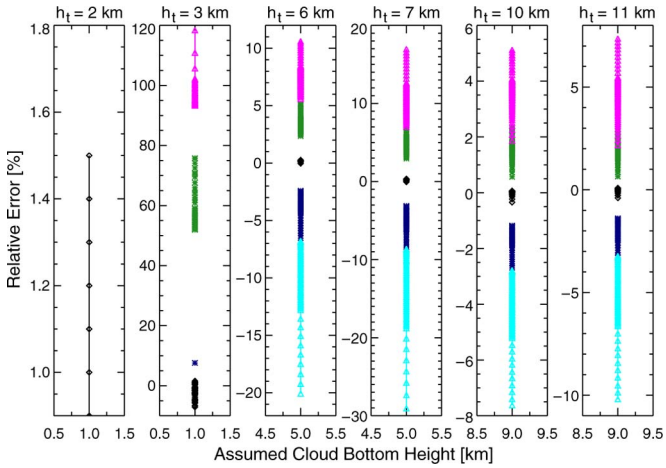

Fig. 7. Relative error in the retrieved cloud bottom height (h_b) related to the cloud optical thickness (τ) retrieval results presented in Figs. 4(b) ($h_b = 1$ km and $h_t = 2$ km), Fig. 5(b) ($h_b = 1$ km and $h_t = 2$ km), Fig. 6(b) ($h_b = 5$ km and $h_t = 6$ km), Fig. 5(c) ($h_b = 5$ km and $h_t = 7$ km), Fig. 6(b) ($h_b = 9$ km and $h_t = 10$ km), and Fig. 6(c) ($h_b = 9$ km and $h_t = 11$ km) at nadir for solar zenith angle equal to 60°. The color code is in accordance with the figures mentioned earlier, i.e., is correlated with the introduced error in cloud top height: (Black) $\Delta h_t = 0$ m, (blue) $\Delta h_t = +100$ m, (green) $\Delta h_t = -100$ m, (cyan) $\Delta h_t = +250$ m, and (magenta) $\Delta h_t = -250$ m. For interpretation of colors, please see online version.

REFERENCES

[1] M. D. King, S. Platnick, P. Yang, G. T. Arnold, M. A. Gray, J. C. Riedi, S. A. Ackerman, and K.-N. Liou, "Remote sensing of liquid water and ice cloud optical thickness and effective radius in the Arctic: Application of airborne multispectral MAS data," *J. Atmos. Ocean. Technol.*, vol. 21, no. 6, pp. 857–875, Jun. 2004.

[2] V. V. Rozanov, M. Buchwitz, K.-U. Eichmann, R. de Beek, and J. P. Burrows, "Sciatran—A new radiative transfer model for geophysical applications in the 240-2400 NM spectral region: The pseudo-spherical version," *Adv. Space Res.*, vol. 29, no. 11, pp. 1831–1835, Jun. 2002.

[3] V. V. Rozanov and A. A. Kokhanovsky, "The solution of the vector radiative transfer equation using the discrete ordinates technique: Selected applications," *Atmos. Res.*, vol. 79, no. 3/4, pp. 241–265, Mar. 2006.

[4] V. V. Rozanov, D. Diebel, R. J. D. Spurr, and J. P. Burrows, "GOMETRAN: A radiative transfer model for the satellite project GOME, the plane-parallel version," *J. Geophys. Res.*, vol. 102, no. D14, pp. 16 683–16 696, Jan. 1997.

[5] H. Bovensmann, J. P. Burrows, M. Buchwitz, J. Frerick, S. Noël, V. V. Rozanov, K. V. Chance, and A. P. H. Goede, "SCIAMACHY: Mission objectives and measurement modes," *J. Atmos. Sci.*, vol. 56, no. 2, pp. 127–150, Jan. 1999.

[6] V. V. Rozanov and A. A. Kokhanovsky, "Semianalytical cloud retrieval algorithm as applied to the cloud top altitude and the cloud geometrical thickness determination from top-of-atmosphere reflectance measurements in the oxygen A band," *J. Geophys. Res.*, vol. 109, no. D5, pp. D05 202-1–D05 202-21, Mar. 2004.

[7] R. B. A. Koelemeijer, P. Stammes, J. W. Hovenier, and J. F. de Haan, "A fast method for retrieval of cloud parameters using oxygen a band measurements from the Global Ozone Monitoring Experiment," *J. Geophys. Res.*, vol. 106, no. D4, pp. 3475–3490, Mar. 2001.

[8] V. V. Rozanov and A. I. Lyapustin, "Similarity of radiative transfer equation: Error analysis of phase function truncation techniques," *J. Quant. Spectrosc. Radiat. Transf.*, vol. 111, no. 12/13, pp. 1964–1979, Aug. 2010.

[9] *Report on the experts meeting on aerosols and their climatic effects*, World Meteorol. Org., Geneva, Switzerland, 1983, Wold Climate Research Program.

[10] V. V. Rozanov, A. V. Rozanov, and A. A. Kokhanovsky, "Derivatives of the radiation field and their application to the solution of inverse problems," in *Light Scattering Reviews*, vol. 2. Berlin, Germany: Springer-Verlag, 2007, pp. 205–265.

[11] V. V. Rozanov and A. V. Rozanov, "Relationship between different approaches to derive weighting functions related to atmospheric remote sensing problems," *J. Quant. Spectrosc. Radiat. Transf.*, vol. 105, no. 2, pp. 217–242, Jun. 2007.

[12] C. D. Rodgers, *Inverse Methods for Atmospheric Sounding: Theory and Practice*, vol. 2. Singapore: World Scientific, 2000, ser. Series on Atmospheric Oceanic and Planetary Physics.